https://scilett-fsg.uitm.edu.my/
Science Letters, **14**(2): 1-14 (2020)
ISSN: 1675-7785
eISSN: 2682-8626
DOI: 10.24191/sl.v14i2.9537

Statistical Optimization for Dye Removal from Aqueous Solution by Cross-linked Chitosan Composite

Ahmed Saud Abdulhameed[1], Ali H. Jawad[2]*, Abdul Karim-Talaq Mohammad[1]

[1]*Chemistry Department, College of Science, University of Anbar, Ramadi, Iraq*

[2]*Faculty of Applied Sciences, Universiti Teknologi MARA (UiTM), 40450 Shah Alam, Selangor, Malaysia*

Corresponding author: ali288@uitm.edu.my / ahjm72@gmail.com

Received: 2 November 2019; Accepted: 5 May 2020; Published: 1 June 2020

ABSTRACT

Response surface methodology-Box–Behnken design (RSM-BBD) was employed to optimize the methyl orange (MO) dye removal efficiency from aqueous solution by cross-linked chitosan-tripolyphosphate/nano-titania composite (Chi-TPP/NTC). The influence of pertinent parameters, i.e. A: TiO_2 loading (0- 50 %), B: dose (0.04-0.14 g), C: pH (4-10), and D: temperature (30-50 °C) on the MO removal efficiency were tested and optimized using RSM-BBD. The F-values of BBD model for MO removal efficiency was 93.4 (corresponding p-value < 0.0001). The results illustrated that the highest MO removal efficiency (87.27 %) was observed at the following conditions: TiO_2 loading (50% TiO_2), dose (0.09 g), pH 4.0, and temperature of 40 °C.

Keywords: *Chitosan; Tripolyphosphate; Nano-titania; Methyl orange dye; Response surface methodology; Adsorption*

INTRODUCTION

Nowadays, synthesis of dyes and their used become in increasing with development different of industries such as textile, plastic, cosmetics, paper, leather and pharmaceuticals [1]. Variety of these dyes are discharged into water and wastewater; therefore, they can be caused serious risks on aquatic life through decreased sunlight penetration that affecting on the photosynthetic activity [2]. Furthermore, dyes can be caused various risks to human such as jaundice, tumors, allergies, cancer, dermatitis, skin irritation and genetic mutations [3]. Therefore, removal of dyes from different kinds of wastewater is necessary to protect environmental system and human health.

There are several methods have been used for removal of dyes such as adsorption [4-6], membrane filtration [7], photocatalytic degradation [8]. Some of these technologies have limitations like less efficient, high working cost, generation of harmful substances and time-consuming [9]. One of the most effective methods used for removal of dyes is adsorption due to its environmentally friendly, simplicity of design and low-

ISSN: 1675-7785
eISSN: 2682-8626
DOI: 10.24191/sl.v14i2.9537

cost [10-12]. Furthermore, generation of harmful substances in the adsorption is reduced compared to others methods [13]. Response surface methodology (RSM) is considered one of the most methods applied to optimize of adsorption process due to reduce the cost and number of experiments as well as giving the information about interaction between the significant factors [14].

One of the most common adsorbent applied for the adsorption is activated carbon due to its high efficiency but it's remain expensive. And for that, the researchers shifted towards natural biopolymers and waste materials as economical alternative adsorbents [15, 16]. Chitosan and chitosan derivatives have been wide applied as adsorbent due to its low-cost, high adsorption capacity and environmentally friendly [17-19]. Use of chitosan as adsorbent in wastewater treatment has some limitations such as low surface area, low mechanical strength, low chemical stability and hydrophobicity [20]. Generally, there are several methods can be utilized for improving the properties of chitosan such as chemical cross-linking reaction and combination of nanoparticles in matrix of chitosan. There are various compounds that utilized as cross-linkers for chitosan such as glutaraldehyde (GLA), tripolyphosphate (TPP), epichlorohydrin {ECH), ethylene glycol diglycidyl ether (EGDE) and glyoxal (GLY) [21-24]. (TPP) is a widely used as ionic cross-linker compound due to its non-toxic, multivalent polyanion, low cost and high solubility in water [25]. Interaction between chitosan and TPP can be occurred through ionic bonding between negative charges of TPP and the positively charged ($-NH_3^+$) of chitosan molecules [26]. In recent years, chitosan-TPP nanoparticles have been prepared and applied in different areas such as wastewater treatment [27], drug delivery [28], medical [29] and food packaging [30].

Titania (TiO_2) particles have several good properties such as high surface area, low-cost, insolubility in water, nontoxicity, commercially available, environmental friendly and high chemical stability [31, 32]. These properties make titania particles is preferred to prepare chitosan/TiO_2 composite and study of their applications. Recently, Chitosan/ titania has been synthesized and used in different applications such as wastewater treatment [33, 34], photocatalysis [35], antimicrobial activity [36], medical applications [37], drug delivery [38], tissue engineering applications [39] and biosensor [40].In this paper, Box-Behnken design (BBD) was applied to optimize the significant parameters for the dye removal (methyl orange, MO) from aqueous solution using hybrid crosslinked chitosan-tripolyphosphate/nano-titania composite (Chi-TPP/NTC). Statistical and graphical of the BBD model were analyzed to obtain on optimum levels of the main effective parameters.

EXPERIMENTAL

Materials

Chi (degree of deacetylation ≥75), nano-titania (type P-25), and TPP solution were supplied from Sigma–Aldrich. MO dye (MW: 327.32, λ_{max} = 464 nm) was obtained from ACROS, Organics. Hydrochloric acid (HCl), acetic acid (CH_3COOH), and sodium hydroxide (NaOH) were supplied from R&M Chemicals. All the reagents and solutions were prepared using ultra-pure water.

Preparation of tripolyphosphate-chitosan/nano-titania composites

The chitosan-tripolyphosphate/nano-titania composite (Chi-TPP/NTC) was prepared based on the method descripted in our previous study [1]. Briefly, 1 g of Chi flakes was added to beaker containing 50 mL of

https://scilett-fsg.uitm.edu.my/
Science Letters, **14**(2): 1-14 (2020)
ISSN: 1675-7785
eISSN: 2682-8626
DOI: 10.24191/sl.v14i2.9537

acetic acid solution (5% v/v) under vigorous stirring at room temperature for 24 h to dissolute of Chi flakes. The viscous solution of Chi was converted to beads form by injection of Chi viscous solution as drops using syringe needle (10 mL) into beaker containing 1000 mL of sodium hydroxide solution (0.5 M). The Chi beads were washed with distilled water to exclude the residual of sodium hydroxide. The crosslinking reaction step was performed by adding of 1% TPP (90 mL) to the Chi beads under slow stirring in water bath for 2 h at 40 °C. After that, the Chi-TPP beads were exhaustedly washed with distilled water. Then, the Chi-TPP was left in an oven for overnight at 80°C and subsequently ground to a uniform particle size (≤ 250 µm) for further study of dye removal properties. A series of Chi-TPP/NTC were prepared by loading two different ratios of TiO_2 particles with Chi (75% Chi:25% TiO_2) and (50% Chi:50% TiO_2) before adding to acetic acid solution. The crosslinking reaction step was performed by same the preparation procedure described above. The Chi-TPP/TNC composite with constant loading ration of (25% TiO_2: 75% Chi) was labeled as Chi-TPP/NTC-25, while the Chi-TPP/NTC composite with constant loading ration of (50% TiO_2: 50% Chi) was labeled as Chi-TPP/TNC-50. The prepared composites were ground to a uniform particle size (≤ 250 µm) for further study of dye removal properties.

Design of experiments

In this work, BBD-RSM was utilized to optimize the effects of four parameters including TiO_2 loading (A), dose (B), pH (C), and temperature on the removal of MO dye onto Chi-TPP/NTC composite surface. The Design Expert 11.0 (Stat-Ease, Minneapolis, USA) was employed for designing of removal tests and statistical analysis of the empirical data. Table 1 displays levels of independent parameters utilized along with their coded values.

Table 1: Coded and actual variables and their levels

Coded variables	Actual variables	Level 1 (-1)	Level 2 (0)	Level 3 (+1)
A	TiO_2 loading (%)	0	25	50
B	Adsorbent dose (g)	0.04	0.09	0.14
C	pH	4	7	10
D	Temperature (℃)	30	40	50

The quadratic polynomial equation was employed to predict the dye removal efficiency and analyze the experimental data as follows (1).

$$Y = \beta_0 + \sum \beta_i X_i + \sum \beta_{ii} X_i^2 + \sum \sum \beta_{ij} X_i X_j \qquad (1)$$

where, Y is the predicted response for MO dye removal (%); X_i and X_j are coded the independent variables; β_0 is the constant; β_i, β_{ii} and β_{ij} are coefficients of linear, quadratic, and interactive coefficient of input independent variables, respectively.

https://scilett-fsg.uitm.edu.my/
Science Letters, **14**(2): 1-14 (2020)
ISSN: 1675-7785
eISSN: 2682-8626
DOI: 10.24191/sl.v14i2.9537

According to BBD, 29 experiments (runs) with three level, four factors and five center points are implemented to optimize and investigate effects of the four parameters i.e. A: TiO_2 loading (0-50 %), B: dose (0.04-0.14 g), C: pH (4-10), and D: temperature (30-50 ºC), on the MO dye removal (%) by Chi-TPP/NTC composite. BBD matrix and obtained response results of MO dye removal (%) are presented in Table 2. A certain amount of adsorbent was taken in a set of Erlenmeyer flasks (125 mL) containing 50 mL of MO dye solution. These flasks were placed in water bath (WNB7-45, Memmert, Germany) and agitated at fixed shaking speed of 100 strokes/min. Then, the adsorbents were excluded from MO dye solutions using syringe filter (0.45 µm). Finally, the MO dye concentrations were measured by UV-Vis Spectrophotometer (HACH DR 2800) at λ_{max} of 464 nm. The percentage of MO dye removal (DR %) was measured as follows (2):

$$DR\ \% = \frac{(C_o - C_e)}{C_o} \times 100 \qquad (2)$$

Where C_o (mg/L) and C_e (mg/L) represent the initial and equilibrium MO concentrations, respectively.

Table 2: The 4-factors BBD matrix and experimental data for MO removal efficiency

Run	A: TiO_2 loading (%)	B: Adsorbent dose (g)	C: pH	D: T (℃)	Dye removal (%)
1	0	0.04	7	40	13.4
2	50	0.04	7	40	25.9
3	0	0.14	7	40	26.8
4	50	0.14	7	40	58.7
5	25	0.09	4	30	57.8
6	25	0.09	10	30	14.8
7	25	0.09	4	50	63.5
8	25	0.09	10	50	18.1
9	0	0.09	7	30	19.5
10	50	0.09	7	30	48.3
11	0	0.09	7	50	22.9
12	50	0.09	7	50	53.8
13	25	0.04	4	40	39.5
14	25	0.14	4	40	68
15	25	0.04	10	40	10.6
16	25	0.14	10	40	21.9
17	0	0.09	4	40	33
18	50	0.09	4	40	87.3
19	0	0.09	10	40	11.7

https://scilett-fsg.uitm.edu.my/
Science Letters, **14**(2): 1-14 (2020)
ISSN: 1675-7785
eISSN: 2682-8626
DOI: 10.24191/sl.v14i2.9537

20	50	0.09	10	40	21
21	25	0.04	7	30	17.3
22	25	0.14	7	30	37.5
23	25	0.04	7	50	20.6
24	25	0.14	7	50	39.4
25	25	0.09	7	40	32.5
26	25	0.09	7	40	32.6
27	25	0.09	7	40	33.5
28	25	0.09	7	40	33.7
29	25	0.09	7	40	33.4

RESULTS AND DISCUSSION

Response surface methodology

Box-Behnken design

The solo and interactive effects of the key parameters such as TiO_2 loading, dose, pH, and temperature on the MO dye removal efficiency were evaluated by BBD-RSM. The relationship of the quadratic polynomial equation between examined parameters and the response (MO dye removal as response) was achieved and showed in the following Eq. (3):

$$\text{MO removal (\%)} = +33.14 + 13.97A + 10.44B - 20.94C + 1.94D + 4.85AB - 11.25AC - 4.22BC - 3.79B^2 + 4.67C^2 \quad (3)$$

where A, B, C and D were the coded levels of TiO_2 loading, adsorbent dose, pH and temperature, respectively.

According to the coefficients of Eq. 3, the parameters including TiO_2 loading, adsorbent dose, and temperature demonstrate a positive impact on MO removal (%) efficiency, while pH had a negative effect [41]. A positive sign in Eq. 3 reveals a synergistic effect of the factors, while a negative sign reveals an antagonistic effect of the factors [42].

Effect of input parameters

The perturbation plot was utilized for investigating the effect of four input parameters simultaneously on the MO removal efficiency as illustrated in Figure 1. As can be seen, there are four key factors responsible for obtaining maximum MO removal efficiency. A sharp curvature for the TiO_2 loading (parameter A) point to that the MO removal efficiency was susceptible to this parameter. Generally, as adsorbent dose (parameter B) increase the MO removal efficiency increases as well. A relatively steep curvature in pH (parameter C) suggests that the MO removal efficiency was sensitive to this parameter. The curve of temperature (parameter D) reveals sensitivity of the response in working temperature levels.

https://scilett-fsg.uitm.edu.my/
Science Letters, **14**(2): 1-14 (2020)
ISSN: 1675-7785
eISSN: 2682-8626
DOI: 10.24191/sl.v14i2.9537

Analysis of variance (ANOVA)

The statistical analysis of the experimental data for the removal MO dye was done using analysis of variance (ANOVA) as shown in Table 3. According to Table 3, the F-value of BBD model and their corresponding p-value are 93.4 and < 0.0001, respectively. This result reveals that the BBD model for the removal MO dye was statistically considerable [43]. Moreover, the coefficient of determination (R^2) value was 0.98, evincing the high correlation between actual and expected MO dye removal values. In general, the terms of BBD model are considered statistically significant when the p-value is less than 0.05 (Prob > F < 0.0500) under selected conditions [44]. Therefore, the BBD model terms of A, B, C, D, AB, AC, B^2, and C^2 were considered statistically significant on the removal MO dye.

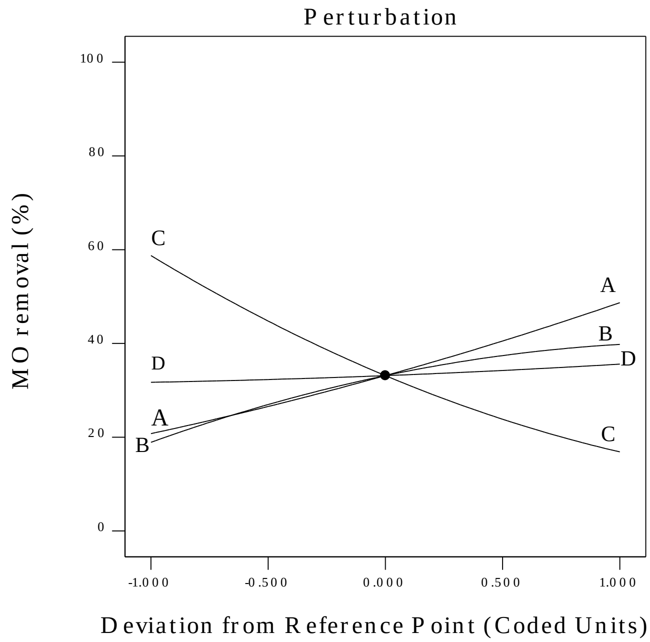

Figure 1: Perturbation plots for the dye removal efficiency of MO. (A) TiO_2 loading, (B) adsorbent dose, (C) pH, and (D) temperature

Table 3: Analysis of variance (ANOVA) of the response surface quadratic model for MO removal efficiency

Source	Sum of Squares	Df	Mean Square	F-value	p-value	Remarks
Model	9933.84	14	709.56	93.40	< 0.0001	S
A-TiO_2 loading	2341.09	1	2341.09	308.15	< 0.0001	S
B-Adsorbent dose	1308.97	1	1308.97	172.29	< 0.0001	S

https://scilett-fsg.uitm.edu.my/
Science Letters, **14**(2): 1-14 (2020)
ISSN: 1675-7785
eISSN: 2682-8626
DOI: 10.24191/sl.v14i2.9537

C-pH	5261.80	1	5261.80	692.58	< 0.0001	S
D-Temp.	44.93	1	44.93	5.91	0.0290	S
AB	94.09	1	94.09	12.38	0.0034	S
AC	506.03	1	506.03	66.61	< 0.0001	S
AD	1.02	1	1.02	0.1343	0.7195	IS
BC	71.06	1	71.06	9.35	0.0085	S
BD	0.5112	1	0.5112	0.0673	0.7991	IS
CD	1.48	1	1.48	0.1943	0.6661	IS
A^2	16.40	1	16.40	2.16	0.1639	IS
B^2	93.18	1	93.18	12.26	0.0035	S
C^2	141.23	1	141.23	18.59	0.0007	S
D^2	1.69	1	1.69	0.2230	0.6440	IS
Residual	106.36	14	7.60			
Cor Total	10040.20	28				

S: Significant; IS: Insignificant

Graphical methods can be also employed to validate the BBD model through evaluation the nature of residuals distribution and correlation between actual and expected MO dye removal values. The normal probability of the residuals in the BBD model can be seen in Figure 2. It can be noticed from Figure 2 that the points demonstrate obvious close to a straight line, indicating the ideal normal distributions and independence of the residuals. The perfect normal distributions of the residuals indicate the accuracy of the assumptions, as well as the independence of the residuals. Plot of the residuals values versus the run number of experiments shows a random distribution around zero indicating the validity of the model [45] as shown in Figure 3.

The relationship between the actual and expected MO dye removal values was presented in Figure 4. The statistical validation of the BBD model can be concluded from Figure 4, where the actual and expected values are close to each other [46, 47]. This close correlation between the actual and predicted values of percentage dye removal was also exhibited by the values of R^2 (0.98) and adjusted R^2 (0.97) which are observed to be close to one**.**

Three-dimensional (3D) response surfaces

Three-dimensional (3D) response surfaces for the MO removal (%) were estimated according to the quadratic model for understanding the responsive relationships between independent parameters and MO removal (%) efficiency. The significant interaction between each two input variables was investigated. The AB interaction was significant (p-value = 0.0034) on MO removal efficiency. Meanwhile, the other parameters (pH 7, and temperature at 40 ºC) were kept constant. The 3-D surfaces and 2-D contours plots for AB interaction are presented in Figure 5a and Figure 5b respectively. Generally, it was found that the MO removal efficiency increases by increasing the TiO_2 loading and adsorbent dose.

https://scilett-fsg.uitm.edu.my/
Science Letters, **14**(2): 1-14 (2020)
ISSN: 1675-7785
eISSN: 2682-8626
DOI: 10.24191/sl.v14i2.9537

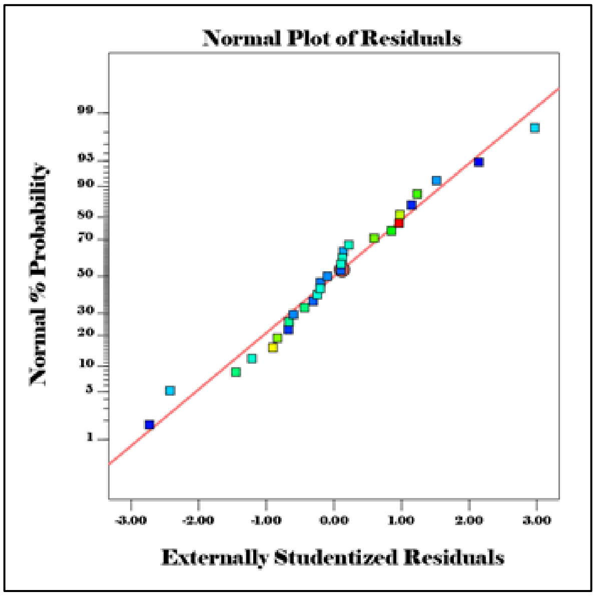

Figure 2: Normal probability plot of residuals for MO removal efficiency.

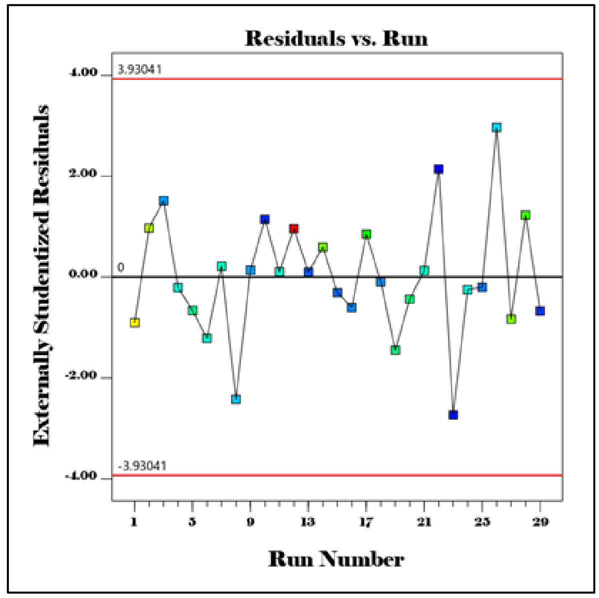

Figure 3: Plot of the residuals values versus run number of experiments.

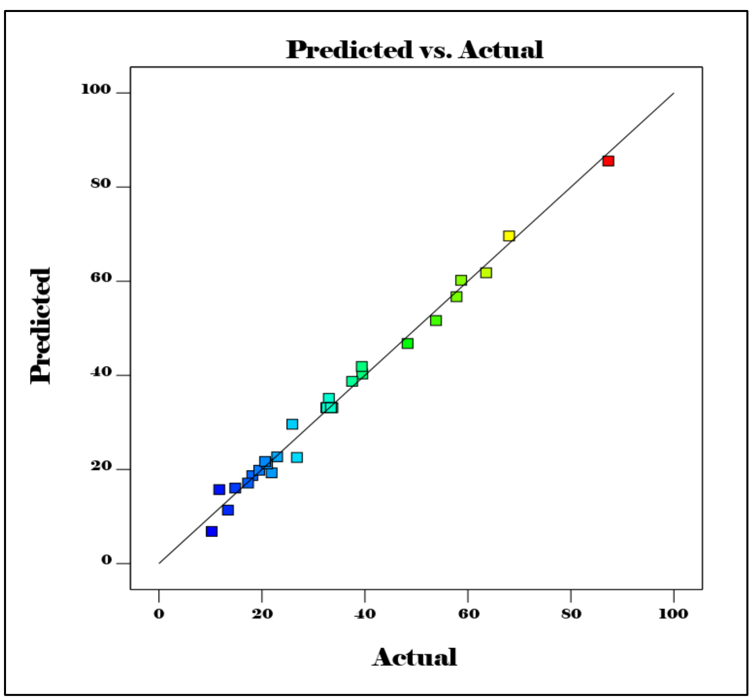

Figure 4: Plot of the relationship between the predicted and actual values of MO removal (%).

https://scilett-fsg.uitm.edu.my/
Science Letters, **14**(2): 1-14 (2020)

ISSN: 1675-7785
eISSN: 2682-8626
DOI: 10.24191/sl.v14i2.9537

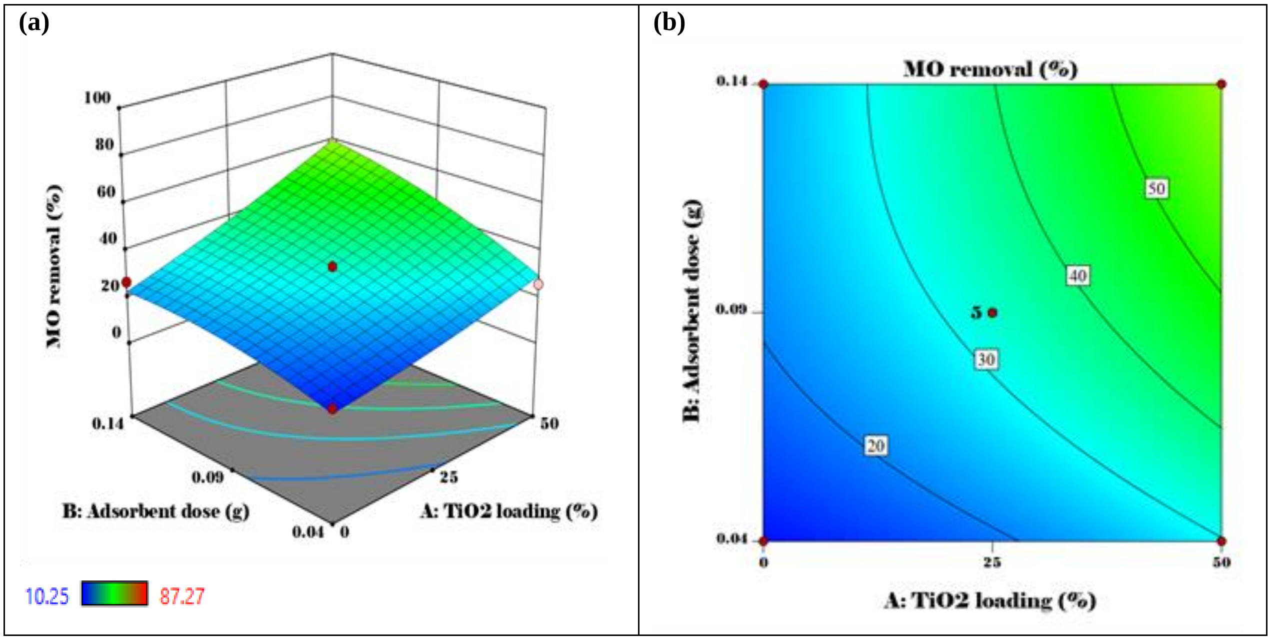

Figure 5: (a) 3D response surface plot and; (b) contour plot for MO removal efficiency showing interaction between TiO_2 loading (A) and adsorbent dose (B).

The remarkable improvement in MO removal efficiency (from 10.25% to 87.27%) with increasing the loading of TiO_2 nanoparticles into crosslinked TPP-chitosan matrix up to 50% chitosan: 50% nano TiO_2. In fact, loading of TiO_2 nanoparticles into polymeric matrix of Chi-TPP will enhance the surface area of Chi-TPP/NTC-50 and introduce new types of hydroxyl groups on the surface Chi-TPP/NTC-50. The terminal hydroxyl and bridging hydroxyl groups on the surface of Chi-TPP/NTC-50 will be protonated and converted to the positive oxonium ions especially in acidic aqueous environment [48, 49].

On the other hand, the sulfonate group ($-SO_3H$) in the molecular structure of the MO can be converted in aqueous medium into active negative sulfonate group ($-SO_3^-$). Consequently, a strong electrostatic (columbic) attraction between positively charged oxonium ions on the surface of Chi-TPP/NTC-50 with negatively charged sulfonate group of MO. Regarding adsorbent dose (B), it is found that the MO removal efficiency increases from 10.25% to 87.27% by increasing Chi-TPP/NTC-50 dose up to 0.09 g/ 50 mL, which can be ascribed to the greater availability of the exchangeable adsorption sites.

The interaction effect of TiO_2 loading (A) and solution pH (C) was significant on MO removal efficiency (p-vaule < 0.0001) as recorded in Table 3. Meanwhile, the other parameters (dose of 0.09 g, and temperature at 40 ^oC) were kept constant. The 3-D surfaces and 2-D contours plots for AC interaction are presented in Figure 6a and 6b, respectively.

From Figure 6, it is observed that the MO removal efficiency increases from 10.25 % to 87.27 % by increasing the maxing ration with TiO_2 nanoparticles from 0% to 50 %, and by decreasing the solution pH from 10 to 4, which can be attributed to the attraction between positively charged oxonium ions on the surface of Chi-TPP/NTC-50 with negatively charged sulfonate group of MO. It was evident that the

https://scilett-fsg.uitm.edu.my/
Science Letters, **14**(2): 1-14 (2020)
ISSN: 1675-7785
eISSN: 2682-8626
DOI: 10.24191/sl.v14i2.9537

maximum MO removal was observed at pH 4, and gradual decreases in the dyes removal can be observed for both dyes by increasing the pH value towards basic environment.

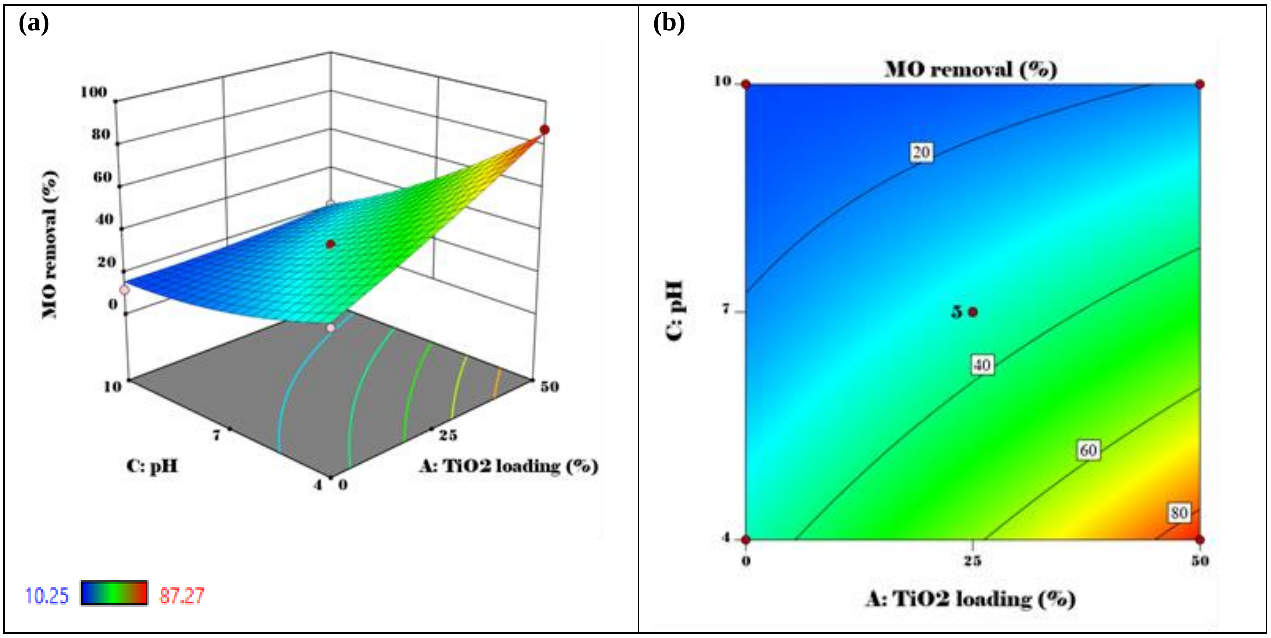

Figure 6: (a) 3D response surface plot; (b) contour plot (b) of MO removal efficiency showing interaction between TiO_2 loading (A) and pH (C).

It was also found that the BC interaction was significant (p-value = 0.0085) on MO removal efficiency. Meanwhile, the other parameters (TiO_2 loading 25 %, and temperature at 40 ^oC) were kept constant. The 3-D surfaces and 2-D contours plots for BC interaction are presented in Figure 7a and 7b, respectively. A positive charge of the Chi-TPP/NTC-50 can be achieved at pH 4, preferring uptake of negatively charged species such as MO. As a result, enhanced electrostatic attractions occur with surface functional groups of positively charged of Chi-TPP/NTC-50 with anionic MO dye denoted in Eq. 4:

$$\mathrm{Chi-TPP/NTC-NH_3^+ + MO-SO_3^- \leftrightarrow Chi-TPP/NTC -NH_3^+ \ldots\ SO_3^- - MO} \qquad (4)$$

CONCLUSIONS

Response surface methodology-Box–Behnken design (RSM-BBD) was successfully utilized as a tool statistical for optimizing the MO dye removal from aqueous solution using crosslinked chitosan composite. The findings demonstrate that the highest MO dye removal (87.27 %) was observed by the following significant interactions: AB, AC and BC. The best conditions of the MO dye removal were TiO_2 loading (50 %), adsorbent dose (0.09g), pH (4), and temperature (40 ^oC).

https://scilett-fsg.uitm.edu.my/
Science Letters, **14**(2): 1-14 (2020)
ISSN: 1675-7785
eISSN: 2682-8626
DOI: 10.24191/sl.v14i2.9537

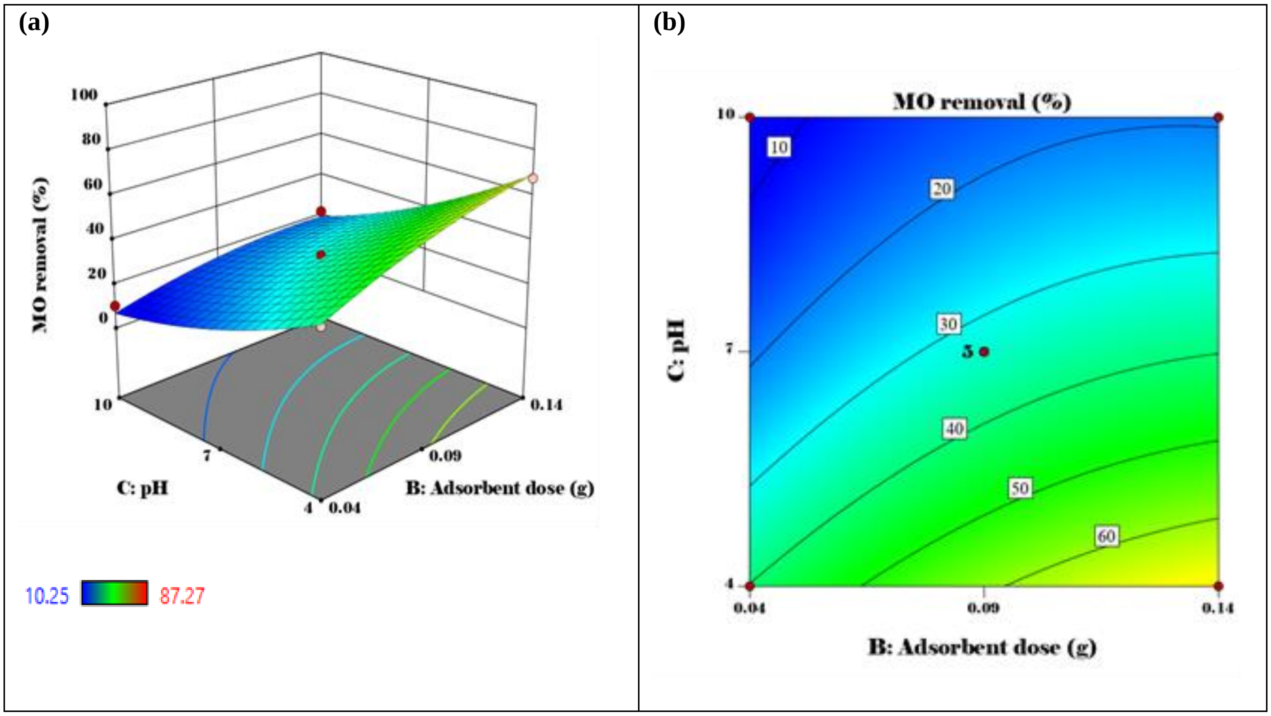

Figure 7: (a) 3D response surface plot, and (b) contour plot of MO removal efficiency showing interaction between adsorbent dose (B) and pH (C).

REFERENCES

[1] A. S. Abdulhameed, A. T. Mohammad, A. H. Jawad, Application of response surface methodology for enhanced synthesis of chitosan tripolyphosphate/TiO_2 nanocomposite and adsorption of reactive orange 16 dye. J. Clean. Prod. 232, (2019) 43-56.

[2] S. Wong, N. A. N. Yac'cob, N. Ngadi, O. Hassan, I. M. Inuwa, From pollutant to solution of wastewater pollution: Synthesis of activated carbon from textile sludge for dye adsorption. Chin. J. Chem. Eng., 26 (2018) 870-878.

[3] J. Dotto, M. R. Fagundes-Klen, M. T. Veit, S. M. Palácio, R. Bergamasco, Performance of different coagulants in the coagulation/flocculation process of textile wastewater. J. Clean. Prod., 208 (2019) 656-665.

[4] A.H. Jawad, A.S. Abdulhameed, M.S. Mastuli, Acid-factionalized biomass material for methylene blue dye removal: a comprehensive adsorption and mechanism study, J. Taibah Univ. Sci. 14(1) (2020) 305-313.

[5] A. S. Abdulhameed, A. T. Mohammad, A. H. Jawad, Modeling and mechanism of reactive orange 16 dye adsorption by chitosan-glyoxal/ TiO_2 nanocomposite: application of response surface methodology, Desalin. Water Treat. 164 (2019) 346-360.

[6] R. A. Rashid, M. A. M. Ishak, K. M. Hello, Adsorptive removal of methylene blue by commercial coconut shell activated carbon. Sci. Lett. 12(1) (2018) 77-101.

[7] R. Ahmad, M. Aslam, E. Park, S. Chang, D. Kwon, J. Kim, Submerged low-cost pyrophyllite ceramic membrane filtration combined with GAC as fluidized particles for industrial wastewater treatment. Chemosphere, 206 (2018) 784-792.

https://scilett-fsg.uitm.edu.my/
Science Letters, **14**(2): 1-14 (2020)

ISSN: 1675-7785
eISSN: 2682-8626
DOI: 10.24191/sl.v14i2.9537

[8] P. B. Santos, J. J. Santos, C. C. Corrêa, P. Corio, G. F. Andrade, Plasmonic photodegradation of textile dye Reactive Black 5 under visible light: a vibrational and electronic study. J. Photochem. Photobiol. A Chem., 37 (2019) 159-165.

[9] M. A. Nawi, S. Sabar, A. H. Jawad, W. W. Ngah, Adsorption of Reactive Red 4 by immobilized chitosan on glass plates: Towards the design of immobilized TiO_2–chitosan synergistic photocatalyst-adsorption bilayer system. Biochem. Eng. J.. 49 (2010) 317-325.

[10] H. M. Rasid, N. Aziz, F. S. A. Ghani, N. Abdullah, Removal of Lead (II) and Chromium (III) from Aqueous Solution by Using Organic-Functionalized MCM-41. Sci. Lett. 14(1) (2020) 23-33.

[11] A.H. Jawad, A.S. Abdulhameed, Mesoporous Iraqi red kaolin clay as an efficient adsorbent for methylene blue dye: Adsorption kinetic, isotherm and mechanism study, Surf. Interfac. 18 (2020) 100422.

[12] S. Karimifard, M. R. A. Moghaddam, Application of response surface methodology in physicochemical removal of dyes from wastewater: A critical review. Sci. Total Environ., 640 (2018) 772-797.

[13] I. M. Lipatova, L. I. Makarova, A. A. Yusova, Adsorption removal of anionic dyes from aqueous solutions by chitosan nanoparticles deposited on the fibrous carrier. Chemosphere, 212 (2018) 1155-1162 .

[14] M. A. Aly-Eldeen, A. A. El-Sayed, D. M. Salem, G. M. El Zokm, The uptake of Eriochrome Black T dye from aqueous solutions utilizing waste activated sludge: Adsorption process optimization using factorial design. Egypt. J. Aquat. Res., 44 (2018) 179-186.

[15] A. S. Abdulhameed, A. H. Jawad, A. T. Mohammad, Synthesis of chitosan-ethylene glycol diglycidyl ether/TiO_2 nanoparticles for adsorption of reactive orange 16 dye using a response surface methodology approach. Bioresour. Technol. 293 (2019) 122071.

[16] Jawad, A. H., Norrahma, S. S. A., Hameed, B. H., & Ismail, K. (2019). Chitosan-glyoxal film as a superior adsorbent for two structurally different reactive and acid dyes: Adsorption and mechanism study Int. J. Biol. Macromol. 135, 2019, 569-581.

[17] S. Sarode, P. Upadhyay, , M. A. Khosa, T. Mak, A. Shakir, S. Song, A. Ullah, Overview of wastewater treatment methods with special focus on biopolymer chitin-chitosan. Int. J. Biol. Macromol.,121 (2018) 1086-1100.

[18] H. He, W. Qi, Y. Fu, M. Zhao, L. Qi, R. Li, Glutaraldehyde non-conjugated chitosan polymer fluorophores for selective determination of picric acid via fluorescence resonance energy transfer strategy. Dyes Pigm., 165 (2019) 25-30.

[19] A.H. Jawad, A.S. Abdulhameed, M.S. Mastuli, Mesoporous Crosslinked Chitosan-Activated Charcoal Composite for the Removal of Thionine Cationic Dye: Comprehensive Adsorption and Mechanism Study, J. Polym. Environ. 28(3) (2020) 1095-1105.

[20] A. H. Jawad, M. A. Islam, B. H. Hameed, Cross-linked chitosan thin film coated onto glass plate as an effective adsorbent for adsorption of reactive orange 16. Int. J. Biol. Macromol. 95, (2017) 743-749.

[21] A. H. Jawad, N. H. Mamat, B. H. Hameed, K. Ismail, Biofilm of cross-linked Chitosan-Ethylene Glycol Diglycidyl Ether for removal of Reactive Red 120 and Methyl Orange: Adsorption and mechanism studies., J. Environ. Chem. Eng., *7* (2019) 102965.

[22] A.H. Jawad, N.S.A. Mubarak, A.S. Abdulhameed, Tunable Schiff's base-cross-linked chitosan composite for the removal of reactive red 120 dye: Adsorption and mechanism study. Int. J. Biol. Macromol. 142 (2020) 732-741.

[23] A. Babakhani, M. Sartaj, Removal of Cadmium (II) from aqueous solution using tripolyphosphate cross-linked chitosan. J. Environ. Chem. Eng. 8 (2020) 103842.

[24] R. V. Pinto, P. S. Gomes, M. H. Fernandes, M. E. Costa, M. M. Almeida, Glutaraldehyde-crosslinking chitosan scaffolds reinforced with calcium phosphate spray-dried granules for bone tissue applications. Mater. Sci. Eng. C 109 (2020) 110557.

[25] L. Bugnicourt, C. Ladaviere, Interests of chitosan nanoparticles ionically cross-linked with tripolyphosphate for biomedical applications. Prog. Polym. Sci., 60 (2016) 1-17.

[26] S. F. Hosseini, M. R. Soleimani, M. Nikkhah, Chitosan/sodium tripolyphosphate nanoparticles as efficient vehicles for antioxidant peptidic fraction from common kilka. Int. J. Biol. Macromol., *111* (2018) 730-737.

[27] E. Alver, M. Bulut, A. Ü. Metin, H. Çiftçi, One step effective removal of Congo Red in chitosan nanoparticles by encapsulation. Spectrochim. Acta A Mol. Biomol. Spectrosc., 171 (2017) 132-138.

https://scilett-fsg.uitm.edu.my/
Science Letters, **14**(2): 1-14 (2020)
ISSN: 1675-7785
eISSN: 2682-8626
DOI: 10.24191/sl.v14i2.9537

[28] B. R. Shah, Y. Li, W. Jin, Y. An, L. He, Z. Li, B. Li, Preparation and optimization of Pickering emulsion stabilized by chitosan-tripolyphosphate nanoparticles for curcumin encapsulation., Food Hydrocoll., 52 (2016) 369-377.

[29] S. Razavi, R. Seyedebrahimi, M. Jahromi, Biodelivery of nerve growth factor and gold nanoparticles encapsulated in chitosan nanoparticles for schwann-like cells differentiation of human adipose-derived stem cells. Biochem. Biophys. Res. Commun., 513, (2019) 681-687

[30] C. Wu, J. Sun, Y. Lu, T. Wu, J. Pang, Y. Hu, In situ self-assembly chitosan/ε-polylysine bionanocomposite film with enhanced antimicrobial properties for food packaging.. Int. J. Biol. Macromol., 132 (2019) 385-392.

[31] A. H. Jawad, M. A. Nawi, Oxidation of crosslinked chitosan-epichlorohydrine film and its application with TiO_2 for phenol removal. Carbohydr. Polym., 90 (2012) 87-94.

[32] A.H. Jawad, N.S.A. Mubarak, A.S. Abdulhameed, Hybrid Crosslinked Chitosan-Epichlorohydrin/TiO_2 Nanocomposite for Reactive Red 120 Dye Adsorption: Kinetic, Isotherm, Thermodynamic, and Mechanism Study, J. Polym. Environ. 28 (2020) 624–637.

[33] A. Razzaz, S. Ghorban, L. Hosayni, M. Irani, M. Aliabadi, Chitosan nanofibers functionalized by TiO_2 nanoparticles for the removal of heavy metal ions. J. Taiwan Inst. Chem. Eng., 58 (2016) 333-343.

[34] A. Jbeli, Z. Hamden, S. Bouattour, A. M. Ferraria, D. S. Conceição, L. V. Ferreira, S. Boufi, Chitosan-Ag-TiO_2 films: An effective photocatalyst under visible light. Carbohydr. Polym., (2018) 199, 31-40.

[35] M. H. Rasoulifard, M. S. Seyed Dorraji, V. Mozafari, Visible light photocatalytic activity of chitosan/poly (vinyl alcohol)/TiO_2 nanocomposite for dye removal: taguchi- based optimization. Environ. Prog. Sustainable Energy, 36 (2017) 66-72.

[36] A. S. Montaser, A. R. Wassel, O. N. Al-Shaye'a, Synthesis, characterization and antimicrobial activity of Schiff bases from chitosan and salicylaldehyde/TiO_2 nanocomposite membrane. Int. J. Biol. Macromol., 124 (2019) 802-809.

[37] S. Samadi, M. Moradkhani, H. Beheshti, M. Irani, M. Aliabadi, Fabrication of chitosan/poly (lactic acid)/graphene oxide/TiO_2 composite nanofibrous scaffolds for sustained delivery of doxorubicin and treatment of lung cancer. Int. J. Biol. Macromol., 110 (2018) 416-424.

[38] Y. Kamari, M. Ghiaci, Preparation and characterization of ibuprofen/modified chitosan/TiO_2 hybrid composite as a controlled drug-delivery system. Micropor. Mesopor. Mat., 234 (2016) 361-369.

[39] R. Jayakumar, R. Ramachandran, V. V. Divyarani, K. P. Chennazhi, H. Tamura, S. V. Nair, Fabrication of chitin–chitosan/nano TiO_2-composite scaffolds for tissue engineering applications. Int. J. Biol. Macromol., 48 (2011) 336-344.

[40] X. Wu, X. Zhong, Y. Chai, R. Yuan, Electrochemiluminescence acetylcholine biosensor based on biofunctional AMs-AChE-ChO biocomposite and electrodeposited graphene-Au-chitosan nanocomposite. Electrochim. Acta, 147 (2014) 735-742.

[41] M. K. Uddin, U. Baig, Synthesis of Co_3O_4 nanoparticles and their performance towards methyl orange dye removal: Characterisation, adsorption and response surface methodology. J. Clean. Prod., 211 (2019) 1141-1153.

[42] F. B. Shahri, A. Niazi, Synthesis of modified maghemite nanoparticles and its application for removal of acridine orange from aqueous solutions by using Box-Behnken design. J. Magn. Magn. Mater., 396 (2015) 318-326.

[43] D. Chen, Y. Li, J. Zhang, W. Li, J. Zhou, L. Shao, G. Qian, Efficient removal of dyes by a novel magnetic Fe_3O_4/ZnCr-layered double hydroxide adsorbent from heavy metal wastewater. . J. Hazard. Mater., 243 (2012) 152-160.

[44] E. Natarajan, G. P. Ponnaiah, Optimization of process parameters for the decolorization of Reactive Blue 235 dye by barium alginate immobilized iron nanoparticles synthesized from aluminum industry waste. Environ. Nanotechnol. Monit. Manage., 7 (2017) 73-88.

[45] A. Z. Moghaddam, E. Ghiamati, A. Pourashuri, A. Allahresani, Modified nickel ferrite nanocomposite/functionalized chitosan as a novel adsorbent for the removal of acidic dyes. Int. J. Biol. Macromol., 120 (2018)1714-1725.

https://scilett-fsg.uitm.edu.my/
Science Letters, **14**(2): 1-14 (2020)

ISSN: 1675-7785
eISSN: 2682-8626
DOI: 10.24191/sl.v14i2.9537

[46] A.H. Jawad, N.N.A. Malek, A.S. Abdulhameed, R. Razuan, Synthesis of Magnetic Chitosan-Fly Ash/Fe_3O_4 Composite for Adsorption of Reactive Orange 16 Dye: Optimization by Box–Behnken Design, J. Polym. Environ. 28(3) (2020) 1068-1082.

[47] N.N.A. Malek, A.H. Jawad, A.S. Abdulhameed, K. Ismail, B.H. Hameed, New magnetic Schiff's base-chitosan-glyoxal/fly ash/Fe3O4 biocomposite for the removal of anionic azo dye: An optimized process. Int. J. Biol. Macromol. 146 (2020) 530-539.

[48] P. A. Nishad, A. Bhaskarapillai, S. Velmurugan, Enhancing the antimony sorption properties of nano titania-chitosan beads using epichlorohydrin as the crosslinker. . J. Hazard. Mater., 334 (2017) 160-167.

[49] A. T. Mohammad, A. S. Abdulhameed, A. H. Jawad, Box-Behnken design to optimize the synthesis of new crosslinked chitosan-glyoxal/TiO_2 nanocomposite: Methyl orange adsorption and mechanism studies. Int. J. Biol. Macromol., 129 (2019) 98-109.